An electron paramagnetic resonance investigation of paramagnetic defects in diamond films grown by chemical vapour deposition

1996 J. Phys.: Condens. Matter 8 837

(http://iopscience.iop.org/0953-8984/8/7/009)

J. Phys.: Condens. Matter **8** (1996) 837–849. Printed in the UK

An electron paramagnetic resonance investigation of paramagnetic defects in diamond films grown by chemical vapour deposition

D F Talbot-Ponsonby†, M E Newton†, J M Baker†, G A Scarsbrook‡, R S Sussmann‡ and C J H Wort‡

† Department of Physics, University of Oxford, Clarendon Laboratory, Parks Road, Oxford OX1 3PU, UK

‡ De Beers Industrial Diamond Division, Charters, Sunninghill, Ascot, UK

Received 19 July 1995, in final form 7 December 1995

Abstract. Defects in free-standing diamond films grown by microwave-plasma-assisted chemical vapour deposition have been studied by electron paramagnetic resonance (EPR). The EPR spectra observed for the as-grown material each consisted of two distinguishable Lorentzian lines at $g = 2.0028(2)$, along with weak satellites centred on $g = 2.0028$ and separated from each other by 1.15–1.35 mT. Comparison of the local concentration (up to 500 ppm) determined by lineshape analysis and the bulk concentration (0.3–8 ppm) determined from the total EPR absorption revealed that the defects were inhomogeneously distributed in the diamond film. Multi-frequency EPR measurements showed that the satellite separation depended on the microwave frequency. It is proposed that the satellite lines originate from a pair of coupled electron spins which form a biradical centre. This appears to be the only model which is consistent with the observed microwave frequency dependence of the satellite separation.

1. Introduction

The synthesis of large areas of free-standing diamond film by chemical vapour deposition (CVD) has been attracting considerable attention over the last decade or so, and currently captivates considerable academic and commercial interest. The quality of the material being produced is improving and it is clear that a thorough understanding of defects in CVD diamond is required.

In this paper, we report a systematic study by electron paramagnetic resonance (EPR) of diamond films grown by microwave-plasma CVD (μw-CVD) under a variety of growth conditions. Several EPR studies on CVD diamond films have been reported in the literature. Watanabe and Sugata [1] reported EPR measurements on diamond films grown by μw-CVD from different starting materials under different conditions. They reported observation of the single-substitutional nitrogen centre [2] ($[N–C]^0$) in some of the films. The $[N–C]^0$ centre is labelled this way because the nitrogen atom substitutes for a carbon atom and forms bonds with three carbon neighbours; the extra electron is localized in an antibonding orbital formed between the nitrogen and the remaining carbon neighbour. It is this carbon which is indicated in the notation $[N–C]^0$ [2, 3]. The superscript indicates the charge of the centre. Watanabe and Sugata [1] also observed an EPR signal at $g = 2.0027(5)$ which appeared to be composed of two components, whose width and intensity varied with the quality of the film.

0953-8984/96/070837+13$19.50

Hoinkis *et al* [4] also reported observation of the $[N–C]^0$ centre in μw-CVD diamond films and Zhang *et al* [5] reported a signal at 2.0028(5) similar to that previously reported [1]. EPR studies on diamond films grown by hot-filament CVD (hf-CVD) revealed the same EPR signal, a symmetrical resonance lineshape which could be deconvoluted into a narrower Lorentzian component and a broader Gaussian component [6]. The g-values of the two resonances were isotropic and equal to 2.0028(2), and the average concentration of paramagnetic centres ranged from 10^{17}–10^{19} cm^{-3}. The average bulk concentrations, linewidths, and relative strengths of the two components were shown to vary with growth conditions [6]. The lineshape analysis is discussed in sections 4.2 and 5. The main conclusion of the lineshape analysis was that in the films studied there was a non-uniform distribution of defects [6].

Jia *et al* [7] reported EPR measurements on diamond films grown using hf-CVD from 99.5% H_2–0.5% CH_4 or similar D_2–CD_4 mixtures. The X-band EPR observed included a central line which appeared to be the sum of a narrow and a broad Lorentzian, both at $g = 2.0028(5)$. In the films grown from 99.5% H_2–0.5% CH_4 satellites were observed at $\pm 0.72(2)$ mT from $g = 2.0028$, whereas no satellites were observed in the films deposited from a similar mixture of D_2–CD_4 or D_2–CH_4. The satellites were attributed to $S = 1/2$ defects hyperfine coupled to adjacent ^{1}H. Their intensity indicated a concentration of about 0.03–0.2 ppm [7], which is only a small fraction of the total ^{1}H concentration measured by NMR to be several thousand ppm [8]. The main lines and the satellites are unaffected by annealing to 1100 °C, but reduced by a factor of approximately 4.5 after 20 min at 1500 °C [7]. ^{1}H NMR studies have indicated that most of the hydrogen resides on crystallite surfaces and is removed by annealing at 850 °C for 2 h [9].

Holder *et al* [10] observed satellites centred on the $g = 2.0028$ EPR transition in CVD films grown by μw-CVD which they attributed to forbidden transitions associated with the simultaneous flipping of an unpaired electron and an environmental proton (weakly coupled to the electron). This proposal is discussed further in sections 4.3 and 5.

It is clear that the $g = 2.0028(5)$ EPR centre is common to CVD diamond grown by different techniques. Satellites are often observed but it appears that their origins may be different for different samples. Here we report multi-frequency EPR measurements on the $g = 2.0028(5)$ centre and satellites observed in μw-CVD diamond films.

2. Experimental details

2.1. Growth and characterization

The free-standing polycrystalline diamond films studied in this paper were grown by microwave-plasma chemical vapour deposition, from a gas mixture of CH_4 and H_2. The general concepts of diamond chemical vapour deposition and growth mechanisms have been reviewed elsewhere [11, 12]. The samples investigated here were prepared under different synthesis conditions to obtain a wide range of material qualities. The material was assessed using Raman, photoluminescence (PL), and infrared absorption and EPR. The Raman and PL spectra were obtained at room temperature with a Reinshaw Ramanoscope with a CCD detection system and excitation with 633 nm light. The infrared absorption measurements were made with a Perkin–Elmer 1710 FTIR spectrometer, at room temperature.

Laser damage testing, and mechanical property and thermal property measurements on bulk polycrystalline CVD diamond have been reported elsewhere [13, 14, 15].

2.2. EPR spectrometers and measurements

Continuous-wave EPR measurements were made at approximately 9.6 GHz and temperatures between 4 and 300 K using a conventional spectrometer and a Bruker TE_{104} cavity. Double integration of the first-harmonic EPR signal and comparison to a reference sample allowed bulk spin concentrations to be determined. The reference used was a synthetic Ib diamond containing EPR-active single-substitutional nitrogen [2], the concentration of which was determined by infrared absorption using the parameters determined by Woods *et al* [16].

Unambiguous interpretation of EPR spectra taken at a single microwave frequency can be very difficult so further EPR measurements were made at 1.2, 1.8, 2.3, 3.5 and 5.8 GHz. The key element for high sensitivity at low microwave frequencies is the loop–gap resonator (LGR) [17]. The LGRs used at the frequencies specified above were single-loop–single-gap devices; microwave coupling was adjusted by varying the separation of the LGR and the coupling loop. The resonators could accommodate a maximum sample diameter of 4.5 mm, and the active length of the LGR was about 10 mm. Measurements were made at temperatures down to 100 K by inserting the LGR into a Varian Q-band nitrogen flow Dewar.

Table 1. The average bulk spin concentration determined by double integration of EPR spectra and comparison to a reference. The relative concentrations of different samples are accurate to ±10%, but the errors on the absolute values are ±20%. The ratio of intensities and linewidths of line X and line Y were determined from simulation. See the text for further details.

Sample No	HWHW 1332 cm^{-1} Raman line (cm^{-1})	1.681 eV PL	Infrared absorption 2760–3030 cm^{-1}
1	4.7(6)	Yes	Very strong
2	5.9(4)	Yes	Strong
3	2.8(6)	Yes	Very weak
4	2.1(2)	Yes	Very weak
5	2.3(2)	Yes	Very weak
6	2.5(1)	Yes	Weak
7	2.3(2)	Yes	Very weak

3. Results

3.1. Raman, PL and infrared absorption

Raman measurements were made at several different points on each side of the CVD diamond film. All of the films exhibited the characteristic first-order Raman peak centred at 1332 cm^{-1}. The peak width varied over the diamond films and an average value for each film is given in table 1. The full width at half-maximum for natural type-IIa diamond is 2.5–3.2 cm^{-1}, and only samples 1 and 2 have a Raman line which is significantly broader. It has been shown that excitation wavelength affects the strength of the Raman signal [18] and wavelengths around 633 to 1060 nm are particularly good at exciting non-diamond phases [19]. In all the samples studied weak broad structure was observed in the range 1200–1600 cm^{-1}, which has been attributed to the presence of double- or triple-bonded carbon [20]. The Raman spectrum for sample 7 is shown in figure 1(a). In the best CVD diamond samples the signal from the non-diamond phases was negligibly small, whereas samples 1 and 2 showed considerable non-diamond structure between 1200 and 1600 cm^{-1}.

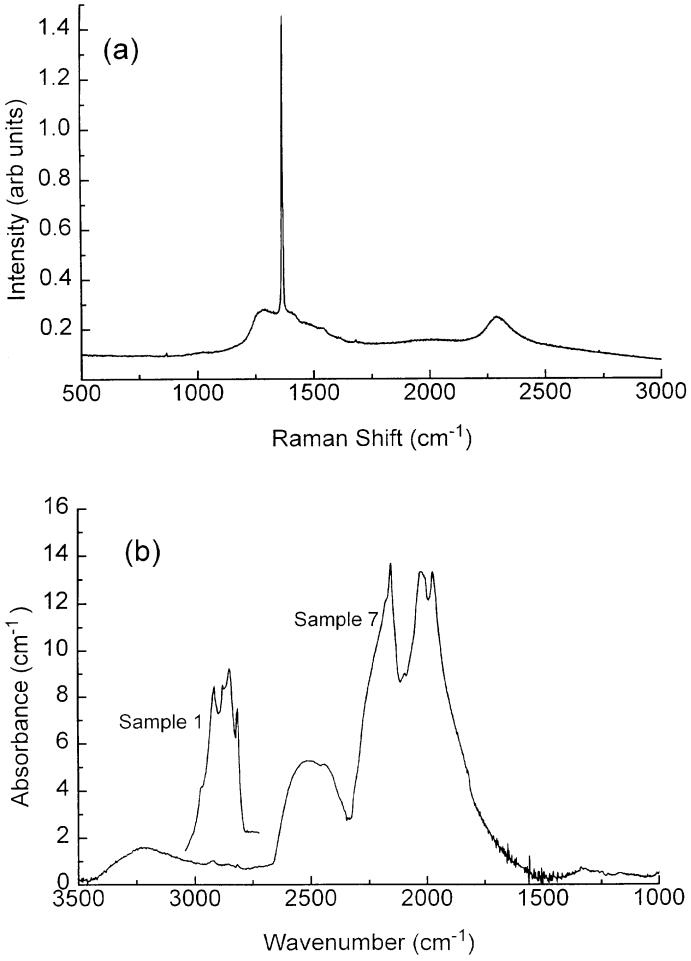

Figure 1. (a) The room temperature Raman spectrum from sample 7 (excitation 633 nm) showing the diamond Raman line at 1332 cm^{-1} and the 1.681 eV photoluminescence feature. (b) The room temperature infrared absorption from sample 7. Note that there is no absorption in the one-phonon region and that there are weak absorption features in the region 2760–3030 cm^{-1}. In the inset we show the infrared absorption of sample 1 in the region 2750–3100 cm^{-1}.

With excitation at 633 nm a PL line centred at 1.681 eV was observed in spectra acquired from all of the samples studied (figure 1(a)). The strength of the 1.681 eV luminescence peak varied markedly over a film; in terms of the concentration of this defect the films are very inhomogeneous. The 1.681 eV defect is believed to involve silicon and is relatively more intense in diamonds containing a high concentration of single-substitutional nitrogen [21]. Wort *et al* [15] report that the presence of the 1.681 eV defect has no bearing on the thermal conductivity or the measured optical properties and by suitable process control the concentration can be reduced below detection limits. The 1.681 eV centre has been unambiguously identified with a silicon impurity, which is probably in a substitutional site and accompanied by a vacancy at a neighbouring lattice site [22].

The infrared absorption spectra from the CVD diamond films showed (as well as the characteristic diamond features) absorption between 3030 and 2760 cm^{-1} which has been

ascribed to C–H stretches on $–CH_2–$ and $–CH_3–$ [23]. In sample 1 (dark CVD) a broad feature is observed between 1000 and 1400 cm^{-1} which has been shown to correlate with the C–H absorption between 2760 and 3030 cm^{-1} [15]. The 2760 to 3030 cm^{-1} absorption is approximately 50% weaker in sample 2 than sample 1 and much weaker in other samples. Figure 1(b) shows the infrared absorption from sample 7.

3.2. EPR studies

We have made EPR measurements on over 40 different polycrystalline CVD diamond films; the results reported here are from films which contain too little single-substitutional nitrogen to be measured using EPR. We estimate that on a typical sample ($10 \times 4.5 \times 0.3$ mm^3) we could measure single-substitutional nitrogen down to a few parts per 10^9. This is two orders of magnitude worse than the spin detection limit of the spectrometer because the $[N–C]^0$ signal typically has a long spin–lattice relaxation time and saturates easily.

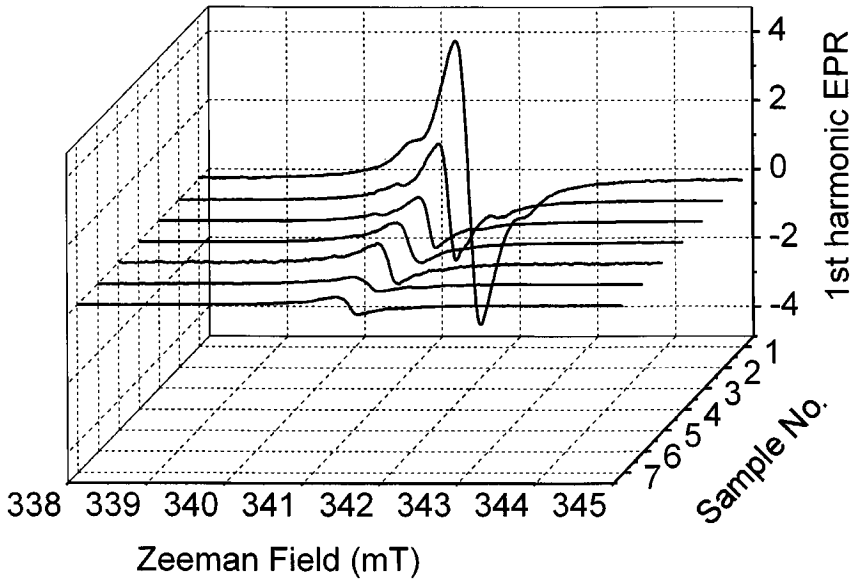

Figure 2. X-band EPR spectra from seven microwave-plasma CVD diamond samples. The microwave frequency was 9.6 GHz and the temperature was 5 K. The spectra have been corrected for sample mass, spectrometer gain and microwave power.

Figure 2 shows X-band (9.6 GHz) EPR spectra from seven different samples taken at a temperature of approximately 5 K. The g-value of the centre of all these spectra is $g = 2.0028(2)$. This has been determined with reference to the $[N–C]^0$ centre ($g = 2.0024(1)$) [2]. The spin concentrations determined from double integration of the EPR spectra and comparison with a reference sample are given in table 2. The spectra shown in figure 2 are unaffected by rotating the sample in the magnetic field. In some samples containing $[N–C]^0$ and the $g = 2.0028$ centre the $[N–C]^0$ centre produces an EPR spectrum expected for a randomly oriented powder; however in others the spectrum depends on the orientation of the magnetic field with respect to the sample showing that the films contain preferentially oriented crystallites. In both randomly and partially oriented films the $g = 2.0028$ resonances and satellites are independent of the orientation of the applied field

Table 2. The average bulk spin concentration determined by double integration of EPR spectra and comparison to a reference. The relative concentrations of different samples are accurate to ±10%, but the errors on the absolute values are ±20%. The ratios of intensities and linewidths of line X and line Y were determined from simulation. See the text for further details.

Sample No	Spin concentration (ppm)	Ratio of intensities line Y/line X	Line X HWHH (mT)	Line Y HWHH (mT)
1	7.7	7.0	0.20	0.59
2	2.1	3.5	0.19	0.69
3	1.0	4.2	0.18	0.67
4	0.8	3.0	0.24	0.68
5	0.8	5.1	0.19	0.61
6	0.4	3.4	0.26	0.75
7	0.3	4.9	0.21	0.64

with respect to the sample.

Figure 3 shows an X-band EPR spectrum from sample 2 which has been simulated by a sum of four Lorentzian lines. In the different samples studied the separation of the satellites at 9.6 GHz varies between 1.15 and 1.35 mT, but the satellites are always centred on $g = 2.0028(2)$. Figure 4 shows the microwave frequency dependence of the separation of satellite lines determined from the second-harmonic EPR spectra of sample 2. The first-harmonic EPR spectra taken from sample 2 at low microwave frequency are shown in figure 5.

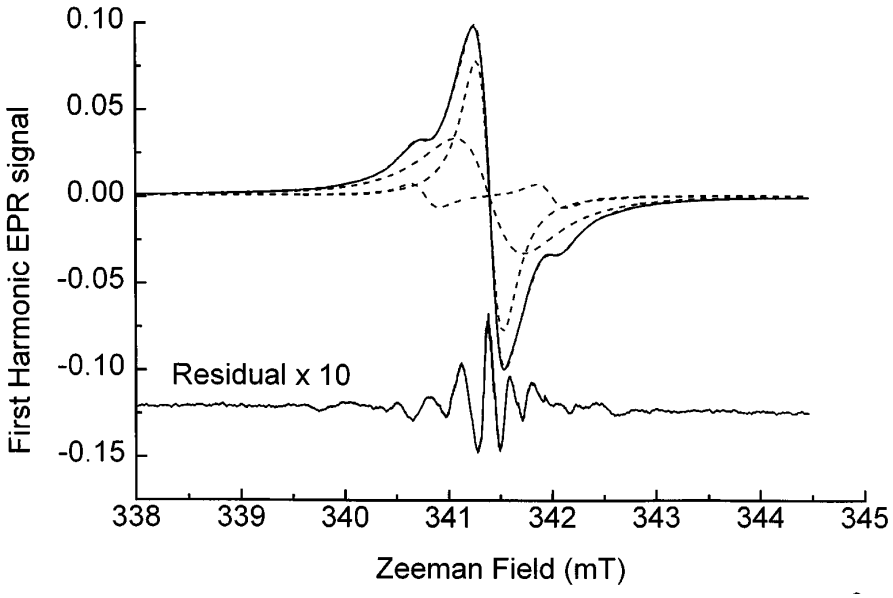

Figure 3. The solid curve shows EPR spectra from sample 2. The microwave frequency was 9.6 GHz, the microwave power was 0.1 mW (TE_{104} cavity), the temperature was 5 K, the modulation frequency was 115 kHz and the modulation amplitude was 0.05 mT. The components of the best fit to four Lorentzian lines are shown as the broken curves. The satellite lines were fixed to have same width and intensity. The residual (experiment minus fit) is shown offset.

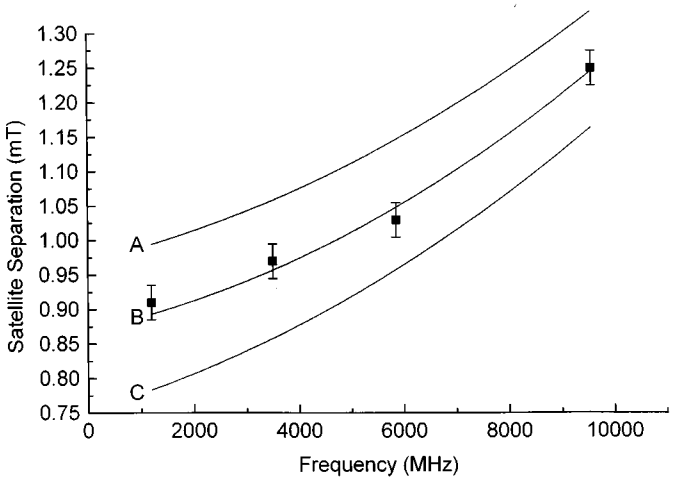

Figure 4. The peak-to-peak separation of satellite lines measured from second-harmonic EPR spectra plotted against the microwave frequency. The solid curves show the satellite separation calculated assuming dipolar coupling between the two electron spins of A: $b_d = -20$ MHz; B: $b_d = -18$ MHz; and C: $b_d = -16$ MHz. Δg = 0.003. See the text for further details.

3.3. Fitting the EPR spectra with a linear combination of Lorentzian lines

The EPR spectra observed in the CVD samples studied here each consist of several overlapping resonances centred at around $g = 2.0028(2)$. Similar results have been reported by other workers for samples grown by different CVD techniques. Least-squares fitting EPR spectra to a sum of Lorentzian, Gaussian and/or Voigt lines is common practice. However, achieving a good fit to a single spectrum is not sufficient—one must proceed with caution and ask several questions.

(i) As the number of components in the fit is increased is the fit really improving?

(ii) Is the lineshape uniquely determined (i.e. does it matter what lineshape we choose?)

(iii) Are the fits of spectra taken at different microwave powers self-consistent?

(iv) Is the temperature dependence of the intensity of the different components sensible (i.e. do they all follow the Curie–Weiss law, or if not is there a reasonable explanation)?

(v) Does the linewidth/shape vary with temperature?

(vi) Are the fits to EPR spectra recorded at different microwave frequencies self-consistent?

The CVD diamond samples studied exhibited a symmetric or very nearly symmetric EPR lineshape; the spectrum in figure 3 is typical. Using a Levenberg–Marquardt χ^2-fitting algorithm [24] the spectrum in figure 3 is satisfactorily reproduced with a combination of four Lorentzian lines (the widths and intensities of the two satellite lines are tied so that a maximum of ten parameters can be simultaneously adjusted). The residual $(y_{expt} - y_{calc})$ is also plotted in figure 3. It is clear from figure 3 and estimations of the goodness of fit using the incomplete gamma function that fit depends strongly on the two central Lorentzians but much less on the satellites. However, it is not possible to reproduce the experimental spectra satisfactorily with only two lines; the satellites must be included.

The narrow Lorentzian saturates with increasing microwave power more rapidly than the broad Lorentzian and the satellites. At room temperature and low microwave power the

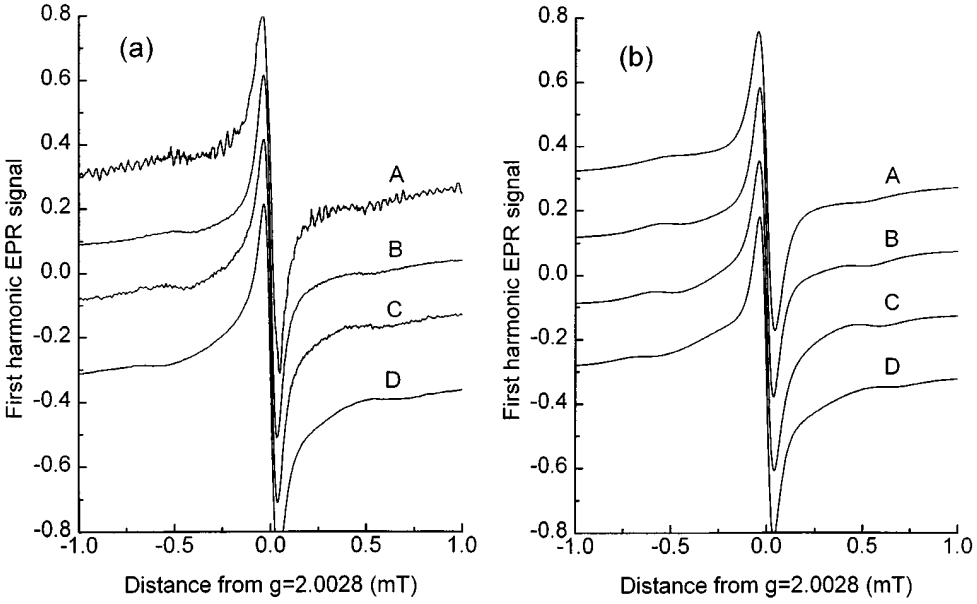

Figure 5. (a) Experimental EPR data from sample 2 taken at 100 K and microwave frequencies of A: 1.1986 GHz; B: 3.496 GHz; C: 5.855 GHz; and D: 9.570 GHz. (b) Simulation of multi-frequency EPR spectra using dipolar coupled biradicals (Δg = 0.003 and $J_{zz} = -36$ MHz) and two Lorentzian lines at microwave frequencies of A: 1.1986 GHz; B: 3.496 GHz; C: 5.855 GHz; and D: 9.570 GHz.

satellites in some samples are effectively invisible because of the relatively large narrow central line. But at low temperatures and high microwave powers, when the narrow Lorentzian is saturated the satellites show up much more clearly.

The relative intensities of the satellites and central lines vary somewhat from sample to sample, but large central lines are associated with large satellites. The separation between the satellite lines varies from 1.15 to 1.35 mT in the films that we have studied. Replacing one or both of the central Lorentzians with Gaussian lines does not result in a satisfactory fit to the experimental data. The quality of the fit is not very sensitive to the shape of the satellite lines.

Fitting the 9.6 GHz EPR data to four Lorentzians reproduces the experimental data reasonably well and the fits remain consistent when the microwave power and temperature are varied. However the separation and relative intensities of the satellites vary with microwave frequency. A different parameter set is required to fit the data at each frequency; clearly the multi-frequency spectra should be fitted in a consistent manner.

4. Discussion

The discussion is separated into three sections: firstly we discuss the origin of the $g = 2.0028$ EPR transition and then in the following two sections analyse the two central lines (section 4.2) and investigate possible explanations for the satellites transitions (section 4.3).

4.1. The origin of the g = 2.0028 EPR line

The nature of the defect responsible for the $g = 2.0028$ EPR transition is uncertain. It is not the negatively charged vacancy which has $g = 2.0027(1)$ [25]. The concentration of vacancies in this charge state is far too low in the samples studied here to explain the concentration of EPR centres. Centres with a single line at $g = 2.0028(6)$ have been observed in neutron- and electron-irradiated diamond [26, 27] and Walter and Estle [28] observed a single-line EPR spectrum with $g = 2.0027(8)$ in crushed diamond. However, there are no models for these defects and we can only speculate that they may be the same as the defect observed in CVD diamond. The $g = 2.0028$ line broadens in samples grown with ^{13}C due to hyperfine coupling with neighbouring ^{13}C atoms [7] but no resolved coupling to ^{13}C or another nucleus has been measured.

The situation is clearly unsatisfactory; we, like others [6, 7], assume that the defect responsible for the $g = 2.0028$ centre is an unpaired electron localized in a carbon dangling bond. The low natural abundance of ^{13}C and the spread of resonant fields in a powder spectrum precludes observation of ^{13}C hyperfine EPR transitions from the central carbon atom.

4.2. The central Lorentzian lines and the distribution of defects

The average bulk spin concentrations given in table 2 were determined by double integration of the EPR spectra and comparison to a reference sample. From the data in table 2 we calculate that the average half-width at half-height of the two central lines over all of the samples is 0.21(3) mT and 0.66(5) mT. The linewidth is independent of temperature and is not determined by the spin–lattice relaxation time (T_1). The linewidth is independent of microwave frequency over the range 1–10 GHz. The Lorentzian shape suggests that the linewidth is not due to strain broadening; we would expect this to produce a Gaussian lineshape.

Magnetic dipolar broadening could account for the width of the EPR lines. Assuming a random distribution of identical paramagnetic centres over a diamond lattice with a probability f that a lattice site is occupied by an unpaired electron, it can be shown that for a single spin species, in the limit of negligible exchange broadening, the second and fourth moments of the absorption lines are

$$M_2 = \frac{3}{5}\left(\frac{\mu_0}{4\pi}\right)^2 g^2\mu_B^2 S(S+1) f \sum_k r_{jk}^{-6} \tag{1}$$

$$M_4 = 3M_2^2\left[0.778 + f^{-1}(0.142 - 0.033(S^2+S)^{-1})\right] \tag{2}$$

where r_{jk} is the separation between the jth and kth unpaired spin, S is the electron spin quantum number and the summation is over all lattice sites. At low concentration both M_2 and M_4 are proportional to the concentration of paramagnetic centres. For $f < 0.01$ the lineshape is compatible with a Lorentzian line, whereas for $f > 0.1$ the lineshape is approximately Gaussian [29]. The concentration of impurities can in principle be determined from M_2 alone. However, for a Lorentzian line numerical evaluation of M_2 leads to a result which is proportional to the cut-off limit of the calculation. This is not a satisfactory approach. It can be shown [29] that the half-width at half-height Δ of a Lorentzian line is given by

$$\Delta = \frac{\pi}{2\sqrt{3}}\sqrt{\frac{M_2^3}{M_4}}. \tag{3}$$

Now Δ can be determined by fitting the EPR spectra and the fractional concentration calculated using equations (1), (2), (3) and the result

$$\sum_k r_{jk}^{-6} = 776 a_0^{-6}$$

where a_0 is the diamond lattice constant. Assuming that the linewidth is predominantly caused by concentration broadening, then linewidths of 0.21 and 0.66 mT indicate unpaired-electron concentrations of approximately 160 and 520 ppm respectively. These values are much higher than the measured bulk concentrations; however, it must be remembered that the estimates based on the linewidth represent a local concentration.

Fanciulli and Moustakas [6] estimated the spin concentrations from a numerical calculation of the second moment evaluated over a range ± 4 mT from the centre of the line. This gave a spin concentration which was several orders of magnitude too small to explain the observed linewidth, which is not surprising because of the underestimation associated with the Lorentzian component. Calculations based on equation (3) appear consistent with the EPR linewidth of the single-substitutional nitrogen centre in synthetic Ib diamond; Δ is positively correlated with the nitrogen concentration [30]. The distribution of nitrogen is in general known to be non-uniform [30]; however, for a uniform distribution equation (3) indicates that $\Delta = 0.2$ mT corresponds to a local concentration of approximately 150 ppm. which is in reasonable accord with our own measurements and the results of Isoya *et al* [30].

The local concentrations determined from the linewidths of the central two Lorentzian lines (X and Y) are consistent with dipolar broadening, but the defect concentration is low enough that the lineshape should remain Lorentzian. There is no need to introduce an exchange interaction; a concentration of paramagnetic defects in a diamond lattice of 500 ppm suggests an average defect separation of about 22 Å. At this separation we would expect the exchange interaction between the spins to be very small. The local defect concentration indicated by the linewidth is one to three orders of magnitude larger than the average bulk concentrations. The results can be reconciled if the majority of the paramagnetic defects are confined to a small region of the CVD diamond film. The observation of two lines of different widths and a low bulk concentration may indicate that the majority of the film is free from paramagnetic defects but there are two other different regions making up less than 2% of the volume of the film which have much higher concentrations of defects. For films 2–7 the ratio of the intensity of lines Y to X varies from 3 to 5.1 (average 4.0, standard deviation 0.8) in a manner uncorrelated with the bulk paramagnetic defect concentration or optical properties. The ratio for film 1, 7.0, is noticeably higher and this film is much darker to the eye than the others.

The high concentrations of paramagnetic defects may be found at grain boundaries or even in included material such as hydrogenated amorphous carbon. The average in equation (1) over the diamond lattice would be inappropriate for these regions and it would be more appropriate to use an alternative average. This would most probably result in a different local concentration. However, this does not alter the fact that the results are consistent with the paramagnetic defects being concentrated in only a small fraction of the volume of the CVD diamond film.

4.3. The origin of the satellites and the biradical defect

In order to correctly interpret the satellites lines seen in figures 2 and 3 we need to consider all of the possible origins of the lines and see which are consistent with the experimental data. Jia *et al* [7] observed satellites separated by 1.44 mT (at the X-band) in diamond films grown by hf-CVD. These satellites were not observed when the H_2 feed gas was replaced

with D_2 and this led the authors to propose that the satellites are ^{1}H hyperfine lines. This interpretation is possibly correct but it would be interesting to confirm the assignment with ^{1}H ENDOR or even multi-frequency EPR to show that the satellite separation is independent of microwave frequency. The separation of the satellites we have observed in the μw-CVD films is dependent on microwave frequency, which means that they are not hyperfine lines.

The satellites do not originate from defects with different g-values. The separation of lines with different g-values is proportional to the microwave frequency, with the separation going to zero as the microwave frequency is reduced. The experimental variation (figure 4) does not follow this dependence.

It was proposed [31, 10] that satellite lines observed in CVD diamond films could result from simultaneous spin flips of an unpaired electron and a weakly coupled proton. This is an appealing proposal because of the interest in determining the presence of hydrogen in CVD diamond films. The forbidden electron–proton spin flips should be separated by approximately $g_N \mu_N B_0$ where g_N is the nuclear g-factor, B_0 the average resonant field for the satellites and μ_N the nuclear magneton. The satellite separations in figure 4 and their intensities do not follow the predictions of this model.

The satellite lines could originate from a pair of coupled electron spins which form a biradical centre. A spin Hamiltonian suitable for a biradical centre in which the spin quantum number S_a and S_b both equal $\frac{1}{2}$ is

$$\mathcal{H} = \mu_B \boldsymbol{S}_a \mathbf{g}_a \boldsymbol{B} + \mu_B \boldsymbol{S}_b \mathbf{g}_b \boldsymbol{B} + \frac{1}{2} (\boldsymbol{S}_a \mathbf{J} \boldsymbol{S}_b + \boldsymbol{S}_b \mathbf{J} \boldsymbol{S}_a) \tag{4}$$

where $\mathbf{g}_a$ and $\mathbf{g}_b$ are the unpaired-electron g-matrices. The coupling matrix $\mathbf{J}$ can include terms arising from isotropic exchange, anisotropic exchange and dipole–dipole interactions. We assume that the matrices $\mathbf{g}_a$, $\mathbf{g}_b$ and $\mathbf{J}$ are symmetric.

Equation (4) contains a maximum of 18 unknown parameters. This is far too many to be determined from the polycrystalline multi-frequency EPR spectra. Therefore we have to make some simplifying assumptions to proceed. We assume that the g-matrices are isotropic, but allow them to have different values. Since the satellite separation is small, we know that unpaired-electron–unpaired-electron interaction is very much less than the Zeeman interaction. In this case if the coupling between the two spins was only due to isotropic exchange then we would expect four transitions, with the separation of the outer satellites (ΔB_{SS}) given by

$$\Delta B_{SS} = \frac{\left[J^2 + (g_a - g_b)^2 \mu_B^2 B_0^2\right]^{1/2} + J}{\langle g \rangle \mu_B} \tag{5}$$

where $\langle g \rangle = \frac{1}{2}(g_a + g_b)$ and $h\nu = \langle g \rangle \mu_B B_0$. The variation in the separation of the satellites in figure 4 can be simulated with equation (5), $\langle g \rangle$ = 2.0028, $\Delta g = |g_a - g_b|$ = 0.003 and $J = 12.8$ MHz. Furthermore, when the biradical spectra are combined with two Lorentzian lines all of the multi-frequency EPR spectra can be well reproduced. However, the exchange coupling is very small and we would reasonably expect to see evidence of anisotropic dipolar coupling. The model invoking only isotropic exchange is difficult to justify; we therefore simulated the satellite separation with $\mathbf{J}$ in equation (4) as being purely dipolar in origin. For a dipolar coupling with $J_{zz} = -36$ MHz, $J_{xx} = J_{yy} = 18$ MHz, $\langle g \rangle = 2.0028$ and $\Delta g = 0.003$ the theoretical variation in satellite separation is shown in figure 4. The experimental variation is well reproduced. When the dipolar biradical spectrum is combined with two Lorentzian lines the multi-frequency EPR spectra are well reproduced; see figure 5. The negative sign was chosen for J_{zz} to be consistent with the

dipolar model. The use of the point dipole model leads to the expression

$$b_d = \frac{1}{3}(J_{zz} - J_{xx}) = -\frac{\mu_0}{4\pi}\langle g\rangle \mu_B R_{ab}^{-3} \tag{6}$$

allowing an estimate to be made of the inter-electron separation R_{ab}. The value of $b_d = -18$ MHz yields $R_{ab} = 14$ Å. This large separation is consistent with a vanishingly small exchange energy and it is likely that the point dipole model will be reasonably accurate.

The dipolar coupled biradical is consistent with the measurements made at all the different microwave frequencies, but is such a defect physically reasonable? We have assumed discrete values of the coupling constants ($g_a = 2.0013$, $g_b = 2.0043$ and $J_{zz} = -36$ MHz) which implies a definite separation of the two spins in the biradical. No lines are observed at the individual g-values, which indicates that these defects can only occur in biradical pairs. The calculated unpaired-electron–unpaired-electron separation is very large (14 Å); it is hard to see why any discrete biradical would be especially stable with such a large separation.

It is very likely that the discrete model is a gross oversimplification of the true system. There is likely to be a spread in the electron–electron separations and the g-matrix of the defect(s) may be anisotropic, so to model the system properly we would need to build into the simulation an average over all possible relative defect orientations as well as a suitably weighted average over the different separations. The wide Lorentzians at $g = 2.0028$ indicate that there are regions of high unpaired-electron concentration where the average unpaired-electron–unpaired-electron separations may approach 20 Å. In such regions even a relatively low concentration of another $S = \frac{1}{2}$ defect with an anisotropic g-matrix could when averaged over the possible orientations and separations give rise to the pair/biradical spectra responsible for the satellites observed. If this defect were only found in regions of high unpaired-electron concentration then no spectra from the isolated radicals would be expected.

5. Conclusion

It appears that the biradical model is the only one which satisfactorily reproduces the variation of the separation of the observed satellites with microwave frequency. The observation of pair/biradical spectra requires either a high concentration of defects such that there is a high probability of finding pairs with a certain mean separation or a specific stable biradical to be formed. The large separation of the unpaired electrons in the pair/biradical estimated from the spacing of the satellite lines suggests that a specific defect is improbable. The broad central Lorentzian lines and the low bulk concentration of paramagnetic defects indicates that there are regions of high unpaired-electron concentration. It is in these regions that the biradical/pair spectra may originate.

In terms of the distribution of paramagnetic centres the films studied here are very inhomogeneous. The multi-frequency EPR studies have shown that the satellite lines in these films are not separate lines with different g-values, allowed hyperfine transitions, or forbidden electron–proton double-spin-flip transitions. X-band EPR investigations alone are not sufficient to unambiguously determine the origin of satellites in polycrystalline CVD diamond films. The fact that satellites have been reported at X-band with separations ranging from 1.12 to 1.44 mT [7, 10] is inconsistent with a specific defect occurring in all CVD samples, but can be easily explained by the biradical model in terms of different average unpaired-electron–unpaired-electron separations in different samples.

Acknowledgments

We thank Professor James S Hyde for allowing us to use the multi-frequency EPR facilities at the National Biomedical ESR Centre, Milwaukee, WI, USA. This facility is supported by the National Institutes of Health grant No RR01008. We are indebted to Dr Andrew Whitehead for sample preparation. This work was supported by EPSRC grant GR/K1562.6. DTP thanks the EPSRC for a studentship and De Beers Industrial Diamond Division for a CASE award.

References

[1] Watanabe I and Sugata K 1988 *Japan. J. Appl. Phys.* **27** 1808
[2] Smith W V, Sorokin P P, Gelles I L and Lasher G J 1959 *Phys. Rev.* **115** 1546
[3] Cox A, Newton M E and Baker J M 1994 *J. Phys. C: Solid State Phys.* **6** 551
[4] Hoinkis M, Weber E R, Landstrass M I, Plano M A, Han S and Kania D R 1991 *Appl. Phys. Lett.* **59** 1870
[5] Zhang W J, Zhang F Q, Wu Q Z and Chen G H 1992 *Mater. Lett.* **15** 292
[6] Fanciulli M and Moustakas T D 1993 *Phys. Rev.* B **48** 14 982
[7] Jia H, Shinar J, Lang D P and Pruski M 1993 *Phys. Rev.* B **45** 17 595
[8] McNamara K M, Levy D H, Gleason K K and Robinson C J 1992 *Appl. Phys. Lett.* **60** 580
[9] Mitra S and Gleason K K 1993 *Diamond Relat. Mater.* **2** 126
[10] Holder S L, Rowan L G and Krebs J J 1994 *Appl. Phys. Lett.* **64** 1091
[11] Bachmann P K, Leers D and Lydtin H 1991 *Diamond Relat. Mater.* **1** 1
[12] Butler J E and Woodin R L 1993 *Phil. Trans. R. Soc.* A **342** 15
[13] Sussmann R S, Scarsbrook G A, Wort C J H and Wood R M 1994 *Diamond Relat. Mater.* **3** 1173
[14] Valentine T J, Whitehead A J, Sussmann R S, Wort C J H and Scarsbrook G A 1994 *Diamond Relat. Mater.* **3** 1168
[15] Wort C J H, Sweeney C G, Cooper M A, Scarsbrook G A and Sussmann R S 1994 *Diamond Relat. Mater.* **3** 1158
[16] Woods G S, Wyk J and Collins A T 1990 *Phil. Mag.* B **62** 589
[17] Froncisz W and Hyde J S 1982 *J. Magn. Reson.* **47** 515
[18] Wagner J, Wild C and Koidl P 1991 *Appl. Phys. Lett.* **59** 779
[19] Wagner J, Wild C and Koidl P 1989 *Phys. Rev.* B **40** 1817
[20] Mermoux M, Roy F, Marcus B, Abello L and Lucazeau G 1992 *Diamond Relat. Mater.* **1** 519
[21] Collins A T, Kamo M and Sato Y 1990 *J. Mater. Res.* **5** 2507
[22] Clark C D, Kanda H, Kiflawi I and Sittas G 1995 *Phys. Rev.* B **51** 16 681
[23] Zhang W, Zhang F, Wu Q and Chen G 1992 *Mater. Lett.* **15** 292
[24] Press W H, Flannery B P, Tenkolsky S A and Vetterling W T 1988 *Numerical Recipes in C* (New York: Cambridge University Press)
[25] Isoya J, Kanda H, Uchida Y, Lawson S C, Yamasaki S, Itoh H and Moriya T 1992 *Phys. Rev.* B **45** 1436
[26] Griffiths J H E, Owen J and Ward I M 1954 *Nature* **174** 439
[27] Faulkner E A and Lomer J N 1962 *Phil. Mag.* B **7** 1995
[28] Walter G K and Estle T L 1961 *J. Appl. Phys.* **32** 1854
[29] Kittel C and Abrahams E 1953 *Phys. Rev.* **90** 238
[30] Isoya J, Kanda H, Norris J R, Tang J and Bowman M K 1990 *Phys. Rev.* B **41** 3905
[31] Newton M E, Cox A and Baker J M 1993 *Diamond Conf. (Bristol, 1993)* ed J E Field (De Beers Industrial Diamond Division) p 1